PROCEEDINGS OF SCIENCE

Study of the radiative tau decays $\tau \to \gamma\ell\nu\overline{\nu}$ with the BABAR detector

Roger Barlow*
University of Huddersfield (GB)
E-mail: roger.barlow@cern.ch

We present measurements of the branching fraction for the radiative τ leptonic decays: $\tau \to \gamma\ell\nu\overline{\nu}$, where the lepton ℓ is either a muon or an electron. The results are obtained from an analysis of the complete *BABAR* data-set consisting of 430 million τ-lepton pairs, corresponding to an integrated luminosity of 468fb^{-1}, collected at the PEP-II asymmetric energy e^+e^- collider at SLAC

The European Physical Society Conference on High Energy Physics
22-29 July 2015
Vienna, Austria

*Speaker.

PoS(EPS-HEP2015)565

1. *BABAR* and PEP-II

Although the PEP-II accelerator and the *BABAR* detector were built for the study of B mesons, a wealth of other physics results has resulted from the high luminosity and the high data quality[1]. Over some ten years of operation $0.5ab^{-1}$ of data was accumulated. Most of this was at the energy corresponding to the rest mass of the $\Upsilon(4S)$, for which the cross section is 1.05 nb; the cross sections for τ pair and charm pair production are comparable, at 0.92 nb and 1.35 nb respectively. Thus the experiment produced some 400 million pairs of τ leptons enabling many measurements to be made of its properties. We here present a recent result on radiative decays. Full details can be found elsewhere[2, 3].

The *BABAR* detector[4] contains several powerful features for the analysis of τ decays: the electromagnetic calorimeter (ECAL) is comprised of 6580 CsI(Tl) crystals, giving excellent energy resolution for the identification and measurement of photons and π^0 particles, and also very efficient and pure electron identification. There is also superb K/π separation from the ring-imaging Cherenkov detector, and precision vertexing.

2. Radiative tau decays

Figure 1 shows the leading order processes that contribute to radiative τ decay (though the second diagram is strongly suppressed).

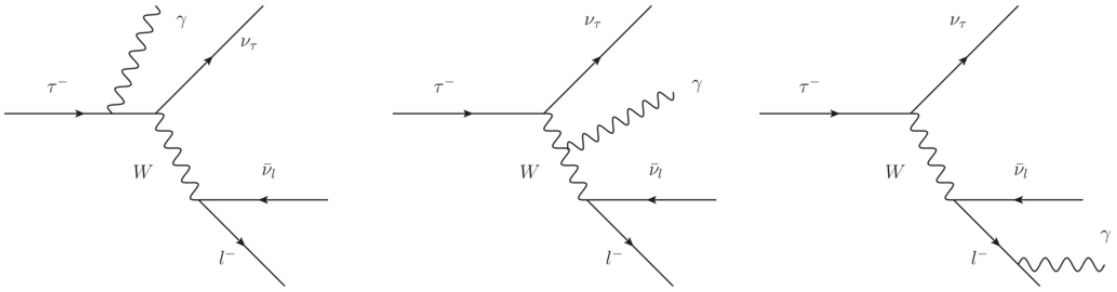

Figure 1: Feynman diagrams for radiative τ decays

In calculating these amplitudes one needs to apply a cutoff to the photon energy as there is an infra-red divergence. In this analysis we consider only events with photons of energy in the τ rest frame is $\omega \geq 10$ MeV as being part of the signal.

A sequence of Monte Carlo programs is used to simulate events: `KK2F` for the pair production of the τ leptons and `Tauola` tau decays. `Photos` is used for radiative corrections in these decays and finally `Geant4` models the response of the detector. This chain is used not only for the usual tasks of calculating the efficiencoes and backgrounds, but also, as it simulates radiative decays down to $\omega = 2MeV$, to find number of $\tau \to \ell\gamma\nu\overline{\nu}$ events with $2 < \omega < 10$ MeV (which, as explained above, are not part of the signal) accepted by the analysis. This number is extremely small, and provides assurance that contamination from $\omega < 2$ MeV decays is negligible.

3. Selection

We use the full 431 fb^{-1} sample of e^+e^- collisions at $\Upsilon(4S)$ energy.

A preliminary selction requires two tracks of opposite charge, both with transverse momentum $p_T > 0.3GeV/c$ and polar angle θ in the range $-0.075 < cos\theta < 0.95$, ensuring they are in the acceptance of the electromagnetic calorimeter. The thrust T is evaluated using all tracks and clusters as $T = max\frac{\sum|\vec{p}_i.\hat{t}|}{\sum p_i}$ and required to lie in the region $0.900 < T < 0.995$. This is a standard way of selecting τ pair evens in *BABAR*, removing $B\overline{B}$ and many hadron continuum events by the lower cut, and light lepton pairs (especially Bhabha scatters) with the upper one.

The thrust axis divides the event into two hemispheres, denoted 'signal' and 'tag' The signal hemisphere is required to contain one track identified as μ or e and exactly one neutral cluster. The tag hemisphere must contain a track, which may be a hadron or a lepton of a different flavour to the signal track. This removes contamination from $\mu^+\mu^-$ and e^+e^- pairs. This hemisphere may also contain additional π^0 photon pairs

As τ decays involve neutrinos and therfore missing energy/momentum, we also require a total visible energy (tracks and clusters) $E_{vis} < 9GeV$, and a total missing transverse mometum $P_T^{miss} > 0.5GeV/c$.

The analysis of the decay to $\mu\gamma\nu\overline{\nu}$ and to $e\gamma\nu\overline{\nu}$ then proceeds separately.

3.1 Muon channel

Muon identification uses a Bagged Decision Tree (BDT) taking as inputs not only the signals in the Instrumented Flux Return (which is the nominal 'muon detector') but also the energy deposited in the electromagnetic calorimeter and $\frac{dE}{dx}$ measured in the tracking. The relevant muon identification efficiency in this analysis is 62 %, with a probability of pion misidentification of approximately 1%

The most important background for this channel arises from muon pairs with initial state radiation from the beam electron and/or positron.

A final selection was made by tuning cuts on four key variables:

$d_{\mu\gamma}$, the distance between the muon track and the photon in the electromagnetic calorimeter.

$cos\theta^*_{\mu\gamma}$, the cosine of the angle between the muon and the photon, in the centre of mass system.

$M_{\mu\gamma}$, the invariant mass of the muon-photon combination.

E_γ, the photon energy, again in the centre of mass system.

The distributions, and the cuts finally chosen, are shown in Figure 2. This gives $15,688 \pm 125$ signal events, with an expected background of $1,596$.

3.2 Electron channel

Electron identification uses an ECOC (Error Correcting Output Code) algorithm, which takes inputs from a set of BDTs, which in turn use inputs from the energy/momentum ratio (as determined by the calorimeter and the tracking chamber respectively), from $\frac{dE}{dx}$ measurements, the shower shape, and other properties. This gives an electron identification efficiency of 91 %, with the probability of pion misidentification below 0.1 %.

The most important background in this channel is from $\tau \to e\nu\overline{\nu}$ decays where the electron undergoes bremsstrahlung in the beam pipe, or other detector component.

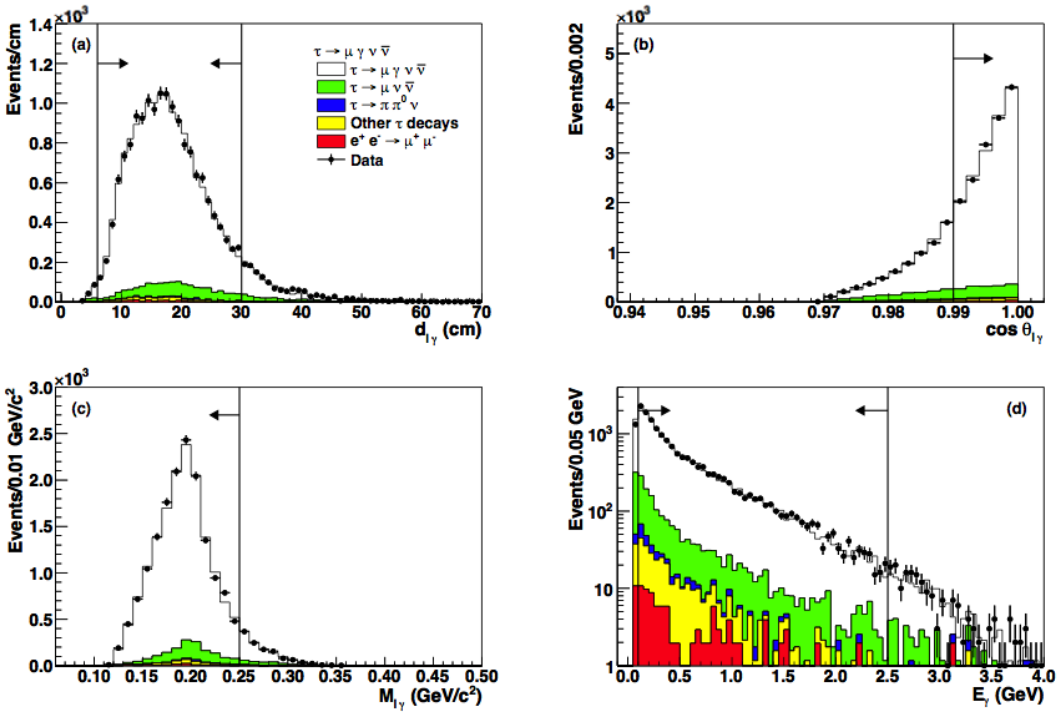

Figure 2: Muon channel: distribution in the four cut variables, with all other cuts applied, showing the data and the expected signal, with the contributions from different backgrounds

The same four quantities were used for the final cuts: $d_{e\gamma}$, $cos\theta^*_{e\gamma}$, $M_{e\gamma}$, and E_γ, defined as for the muon channel. The distributions and the optimised cut values are shown in Figure 3. (The cut values are very different for the two channels due to the different nature of the important background.) This gives $18,149 \pm 135$ signal events with an expected background of 2,823.

3.3 Optimisation

In such selections cuts are tuned to maximise the expected signal S and minimise the expected background B: two objectives which are, in general, not compatible. The normal technique when making a measurement (as opposed to setting a limit) is to maximise the ratio $\frac{S}{\sqrt{S+B}}$, thereby minimising the fractional statistical error on the measured value. However in an analysis such as this the statistical errors are very small, and systematic errors are important. The tuning of the cuts should be done to minimise the fractional total error, combining both statistical and systematic contributions.

The measured branching ratio BR is obtained from N, the number of events that survive the cuts

$$BR = \frac{N - B}{2\varepsilon\sigma\mathscr{L}}$$

The cross section for τ pair production, σ, and the integrated luminosity, $\mathscr{L}$, are not effected by the cuts, but the background B and the efficiency ε are. We assume that these systematic errors

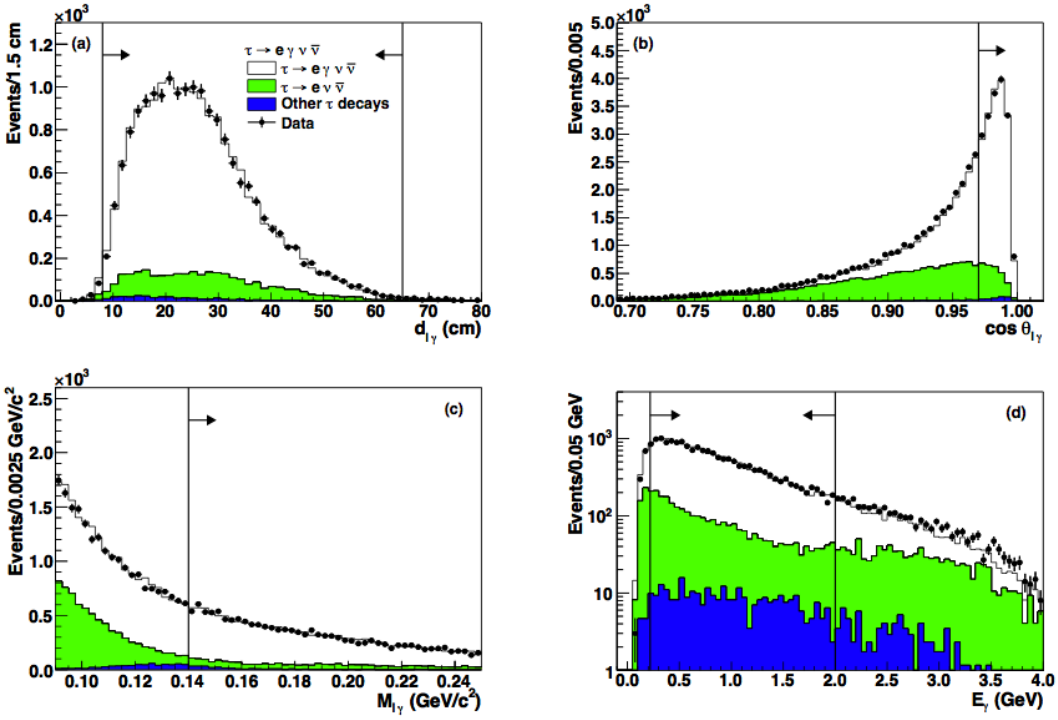

Figure 3: Electron channel: distribution in the four cut variables, with all other cuts applied, showing the data and the expected signal, with the contributions from different backgrounds

are proportional to the actual values

$$\sigma_B = \alpha B, \qquad \sigma_\varepsilon = \beta\varepsilon$$

a model which covers many situations, including the one here. If these errors are included then the figure of merit, to be maximised, becomes

$$\frac{S}{\sqrt{S+B+\alpha^2B^2+\beta^2}}$$

Use of this method favours harsher cuts, with lower backgrounds, giving smaller total errors. In our case, standard optimisation would give much larger signals, 50,517 μ and 531,765 e decays, with very much larger backgrounds of 25,264 and 993,417 respectively.

4. Systematic uncertainties

The evaluated contribution to the systematic errors for the two channels are shown in Table 1. The values are uncertainties on correction factors that are mostly obtained from the data itself, for example the photon efficiency is found by identifying acolinear muon pairs for which energy-momentum conservation requires that a photon was emitted, and then looking in the calorimeter to see whether such a photon was found.

	μ channel uncertainty (%)	e channel uncertainty (%)	method
Photon efficiency	1.8	1.8	$\mu^+\mu^-\gamma$ and π^0 effcy from $\tau \to \pi\nu/\tau \to \rho\nu$ ratio
Particle ID	1.5	1.5	$\mu\mu\gamma$ and $ee(\gamma)$ for effcy
Background	0.9	0.7	$\tau^\pm \to \pi^\pm\pi^+\pi^-\nu$
BF	0.7	0.7	PDG
L and cross section	0.6	0.6	standard value
MC statistics	0.5	0.6	
Selection criteria	0.5	0.5	comparisons
trigger selection	0.5	0.6	comparisons
Track reconstr.	0.3	0.3	standard value
Total	2.8	2.8	Sum above in quadrature

Table 1: Systematic errors

	$B(\tau \to \mu\gamma\nu\overline{\nu})$	$B(\tau \to e\gamma\nu\overline{\nu})$
OPAL[5]	$(3.0 \pm 0.4 \pm 0.5) \times 10^{-3}$	
CLEO[6]	$(3.61 \pm 0.16 \pm 0.35) \times 10^{-3}$	$(1.75 \pm 0.06 \pm 0.17) \times 10^{-2}$
BABAR	$(3.69 \pm 0.03 \pm 0.10) \times 10^{-3}$	$(1.847 \pm 0.015 \pm 0.052) \times 10^{-2}$
SM - LO[7]	3.67×10^{-3}	1.84×10^{-2}
SM - NLO[8]	$(3.572 \pm 0.003 \pm 0.006) \times 10^{-3}$	$(1.645 \pm 0.019 \pm 0.003) \times 10^{-2}$

Table 2: Results of our measurements, and comparison to previous experiments and theoretical predictions

5. Results

Table 2 shows our results, with those from OPAL and CLEO (OPAL used ω of 20 MeV rather than 10 MeV so this is not directly comparable, but the difference is very small) and the theoretical predictions. The Standard Model calculations at Next to Leading Order (NLO) are very recent. Errors quoted are split into uncertainty from NNLO etc and from the τ lifetime.

The data agree with the leading order predictions, but for NLO there is a 3.5 σ disagreement for the electron channel (though good agreement for muons). This may be due to the calculation's 'exclusive' requirement: that only one photon exceeds 10 MeV threshold. Their 'Inclusive' prediction is higher (1.728×10^{-2}) . Our case is intermediate in that a decay with two photons of, say, 100 and 200 MeV would indeed not be selected, but with 100 and 11 MeV it probably would .

6. Conclusions

We have measured the branching fractions for the radiative decays of the τ lepton to be:
$BF(\tau^\pm \to \mu^\pm\gamma\nu\overline{\nu}) = (3.69 \pm 0.03 \pm 0.10) \times 10^{-3}$
$BF(\tau^\pm \to e^\pm\gamma\nu\overline{\nu}) = (1.847 \pm 0.015 \pm 0.052) \times 10^{-2}$.

Our result is much more precise than previous measurements, in both the statistical and the systematic error. As such it provides an interesting test of electroweak calculations

References

[1] A Bevan *et al.*(Ed.) *The Physics of the B factories* Eur. Phys. J C 74:3026 (2014)

[2] Benjamin Oberhof: *Measurement of $\mathscr{B}(\tau \to \ell\nu\overline{\nu}), \ell = e, \mu$ at BABAR*). PhD Thesis, University of Pisa (2015)

[3] J.P.Lees *et al.*, (The *BABAR* collaboration) *Measurement of the branching fractions of the radiative leptonic τ decays $\tau \to e\gamma\nu\overline{\nu}$ and and $\tau \to \mu\gamma\nu\overline{\nu}$ at BABAR.* Phys. Rev. D. Rapid Communication **PRD-RC 91**, 051103 (2015)

[4] B. Aubert *et al.*, (The *BABAR* collaboration) *The BABAR Detector* Nucl.Instrum.Meth.A479:1-116, (2002)

[5] G. Alexander *et al.*, (The OPAL collaboration) Phys. Lett. B388, 437 (1996).

[6] T. Bergfeld *et al.*, (The CLEO collaboration) Phys.Rev.Lett. 84, 830-834, (2000).

[7] M. Fael, L. Mercolli and M. Passera *W propagator corrections to muon and tau leptonic decays*, Phys. Rev. D 88 093011 (2013)

[8] M. Fael *et al.*, *Radiative μ and τ leptonic decays at NLO*, arXiv 1506.03416 (2015)